1972

The electric field strength dependence of neutron-induced defects in silicon P-N junctions

Paul Edward Johnson

Department:

THE ELECTRIC FIELD STRENGTH DEPENDENCE OF NEUTRON-INDUCED DEFECTS IN SILICON P-N JUNCTIONS

BY

PAUL EDWARD JOHNSON, 1944-

A THESIS

Presented to the Faculty of the Graduate School of the

UNIVERSITY OF MISSOURI-ROLLA

In Partial Fulfillment of the Requirements for the Degree

MASTER OF SCIENCE IN METALLURGICAL ENGINEERING

1972

Approved by

Charles A. Gibson (Advisor) Fred C. Glandus

Albert E. Bolon

ABSTRACT

The effect of high electric field strengths (10^4 to 10^5 V/cm) present during neutron radiation on the neutron-induced defects is determined by utilizing the high electric field strength inherent in the emitter-base transistion region of an n-p-n transistor. A method is presented for the separation of neutron and gamma effects. Previous theoretical work on the ratio of base current increase to collector current decrease is applied to experimental data. The variations of the space-charge region volume damage introduction rate with neutron fluence and the average electric field strength are determined experimentally in order to obtain a measure of this effect. The dependence of the space-charge region volume damage introduction rate on neutron fluence is found empirically to be a power law relationship. The space-charge region volume damage introduction rate is shown empirically to also have a power law relationship with respect to the average electric field strength.

TABLE OF CONTENTS

LIST OF ILLUSTRATIONS

LIST OF TABLES

I. INTRODUCTION

Neutron-induced defect clusters in silicon transistors have been shown[1-6] to behave differently in the high electric field strength emitter-base space-charge region than in the low electric field strength "neutral" bulk-base region both during introduction and annealing[5]. This anomalous behavior in both formation and annealing has been attributed by some authors to carrier density effects[7] or to a modification of the defect cluster or its capture cross-section by the presence of an electric field[5,6].

The purpose of the investigation reported here was to determine if such an electric field strength dependence existed through a study of the variation of the space-charge volume damage introduction rate, K_V, with junction electric field strength, E, and neutron fluence, Φ. Two groups of devices, whose emitter-base junctions were forward biased, unbiased, and reverse biased in order to alter the junction electric field strengths, were irradiated with fast neutrons (E>10keV, fission source). The rate of introduction of total space-charge volume damage and surface damage, K_{tot}, was then computed from changes in base current for each device after accounting for the neutron-induced recombination in the neutral bulk region. The gamma-induced surface recombination and the neutron-induced space-charge recombination were then extracted from these total space-charge volume and surface damage rates. The rate of space-charge damage introduction was observed to be a function of the

neutron fluence. The rates of space-charge damage introduction were then compared and an electric field strength dependence of the space-charge volume damage introduction rate was also found to exist.

II. BACKGROUND OF THE PROBLEM

The space-charge region neutron-induced base current component, $I_{B\Phi}$, which is primarily responsible for degradation of silicon device current gain at low and intermediate current/injection levels through degradation of the emitter efficiency, is related to the rate of space-charge volume damage introduction, K_V, by the expression[6],

$$\Delta I_{B\Phi} = K_V \cdot X_m(V_{BE}, \Phi) \cdot \Phi \cdot A_E \cdot \exp(qV_{BE}/nkT) \quad (1)$$

where

$\Delta I_{B\Phi}$ = space-charge region neutron-induced base current increase (A),

A_E = effective emitter area (cm^2),

K_V = rate of space-charge region volume (S-CRV) damage introduction ($A \cdot cm^{-3}$/neutron cm^{-2}),

Φ = neutron fluence (neutrons/cm^2, E>10keV),

q = electronic charge (1.609×10^{-19} coulombs),

n = reciprocal slope term $\simeq$ 1.5 (see Equation (14)),

k = Boltzman's constant (8.63×10^{-5} eV/°K),

T = temperature (°K),

X_m = base-emitter depletion layer width (cm),

V_{BE} = base-emitter bias (V),

The magnitude of the neutron-induced space-charge component of base current, $I_{B\Phi}$, the voltage dependence of this component (i.e., the reciprocal slope term, n), and the volume of the emitter-base space charge region, $A_E \cdot X_m$, must be determined in order to obtain the dependence of the

rate of the space-charge volume damage introduction, K_V, on neutron fluence.

The base current is composed of several current components as shown in Figure 1a. Direct measurement of the neutron-induced space-charge current component is not possible over more than two to three decades of the device operating range. At low and intermediate current/injection levels the changes in only three base-current components dominate the total base current change. The first of these is the neutron-induced space-charge recombination-generation current, the second is the neutron-induced neutral bulk base region recombination-generation current, and the third is the gamma-induced surface recombination-generation current.

The neutron-induced space-charge component dominates the base current changes at low fluences and low to intermediate current injection levels[1-4]. The neutron-induced neutral base component becomes important at higher fluences and current/injection levels[4,9]. A mathematical model for the base region of graded base devices has been developed[4,9]. This model predicts that the rate of increase in the neutral base region recombination current component with neutron fluence is generally greater than and directly proportional to the observed and readily measured decrease in the collector current.

The earlier experiments[1-4] were performed at the Sandia Pulsed Reactor Facility (SPRF) which has a very low gamma-to-neutron ratio. The University of Missouri-Rolla Research

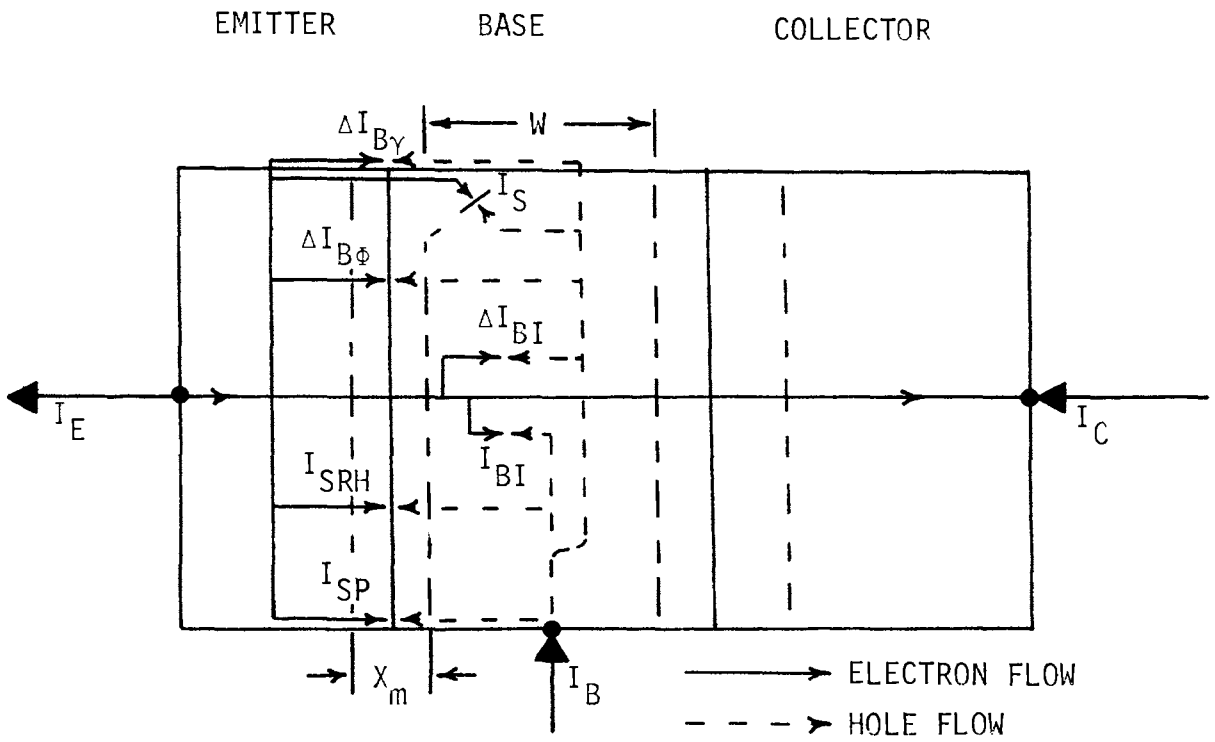

NORMAL BASE CURRENT COMPONENTS (A)

ORIGIN	VOLTAGE DEPENDENCE
I_{SP}-EMITTER PERIMETER JUST BELOW THE SURFACE	exp(qV/mkT), m≈1.5
I_{SRH}-EMITTER-BASE SPACE-CHARGE REGION	exp(qV/mkT), m<2.0
I_{BI}-BULK BASE REGION	exp(qV/kT)

NEUTRON-INDUCED BASE CURRENT COMPONENTS (A)

ΔI_{BI}-BULK BASE REGION	EQUAL TO $r \cdot \Delta I_C$
$\Delta I_{B\Phi}$-EMITTER-BASE SPACE-CHARGE REGION	exp(qV/nkT), n≈1.5

GAMMA-INDUCED BASE CURRENT COMPONENTS (A)

$\Delta I_{B\gamma}$-EMITTER PERIMETER AT THE SURFACE	exp(qV/mkT), m<2.0
I_S-SURFACE CHANNEL	exp(qV/mkT), 2<m<4 for Si

Figure 1a. Origins of the normal and radiation-induced recombination-generation current components in a silicon N-P-N transistor.

Reactor used in this group of experiments has a gamma-to-neutron ratio of 1.14×10^{-8} rads(Si)/(neutrons/cm^2)[10]. Consequently, it is necessary to separate the gamma-induced surface current component from the base current change in order to study the bulk effects.

The fraction of the total base current which originates in the emitter-base space-charge volume attributed only to neutrons, $\Delta I_{B\Phi}$, may be calculated over a wide range of current/injection levels by correcting the total current change with irradiation for the gamma-induced surface current and the neutron-induced "neutral" base region current (using the proportionality to the decrease in collector current). The expression for this operation may be written as,

$$\Delta I_{B\Phi}(V_{BE},E,\Phi) = \Delta I_{Btot}(V_{BE},E,\Phi,\gamma) - R \cdot \Delta I_C(V_{BE},\Phi) - I_{BS} \cdot f(E,\gamma) \qquad (2)$$

where

ΔI_{Btot} = total measured change in the base current caused by the introduction of the neutron-induced bulk space-charge recombination current plus the neutron-induced increase in the "neutral" base recombination current and the gamma-induced surface current (A),

ΔI_C = measured decrease in the collector current caused by the neutron-induced increase in the "neutral" base region recombination (A),

R = ratio of increase in the neutral-base region

current component to decrease in collector current[4,9].

$I_{BS} \cdot f$ = empirical expression for the addition of surface currents in terms of the initial surface component of base current and the electric field strength present during irradiation[10,11](A),

E = average junction electric field strength (V/cm), and

γ = gamma dose (rads(Si)).

A preliminary experiment was performed to determine whether an electric field strength dependence of K_V did in fact exist. Three Motorola 2N914 transistors were matched to within 10% using as references the zero bias capacitance and collector and base currents measured over the range of emitter-base bias from 0.2 to 0.7 volts. These three devices were irradiated in one step to a neutron fluence of 2×10^{14} neutrons/cm^2 (E>10keV). During this irradiation, one device was forward biased at 0.5 V to reduce the average built-in electric field strength to 5.2×10^4 V/cm, one device was at zero bias to leave the average built-in electric field strength at 6.6×10^4 V/cm, and one device had a 3 V reverse bias to produce an average electric field strength of 1.5×10^5 V/cm. The S-CRV damage introduction rate was calculated using Equation (1), with V_{BE} equal to 500 mV forward bias[6]. The values obtained were 4.1×10^{17} (A/cm^3)/(neutrons/cm^2) for the forward biased device,

5.1×10^{-17} for the zero biased device, and 10.6×10^{-17} for the reverse biased device. In Figure 1 these values are plotted versus the average electric field strength during irradiation. The results of this experiment clearly indicate the existence of an electric field dependence of the volume damage introduction rate for the space-charge region.

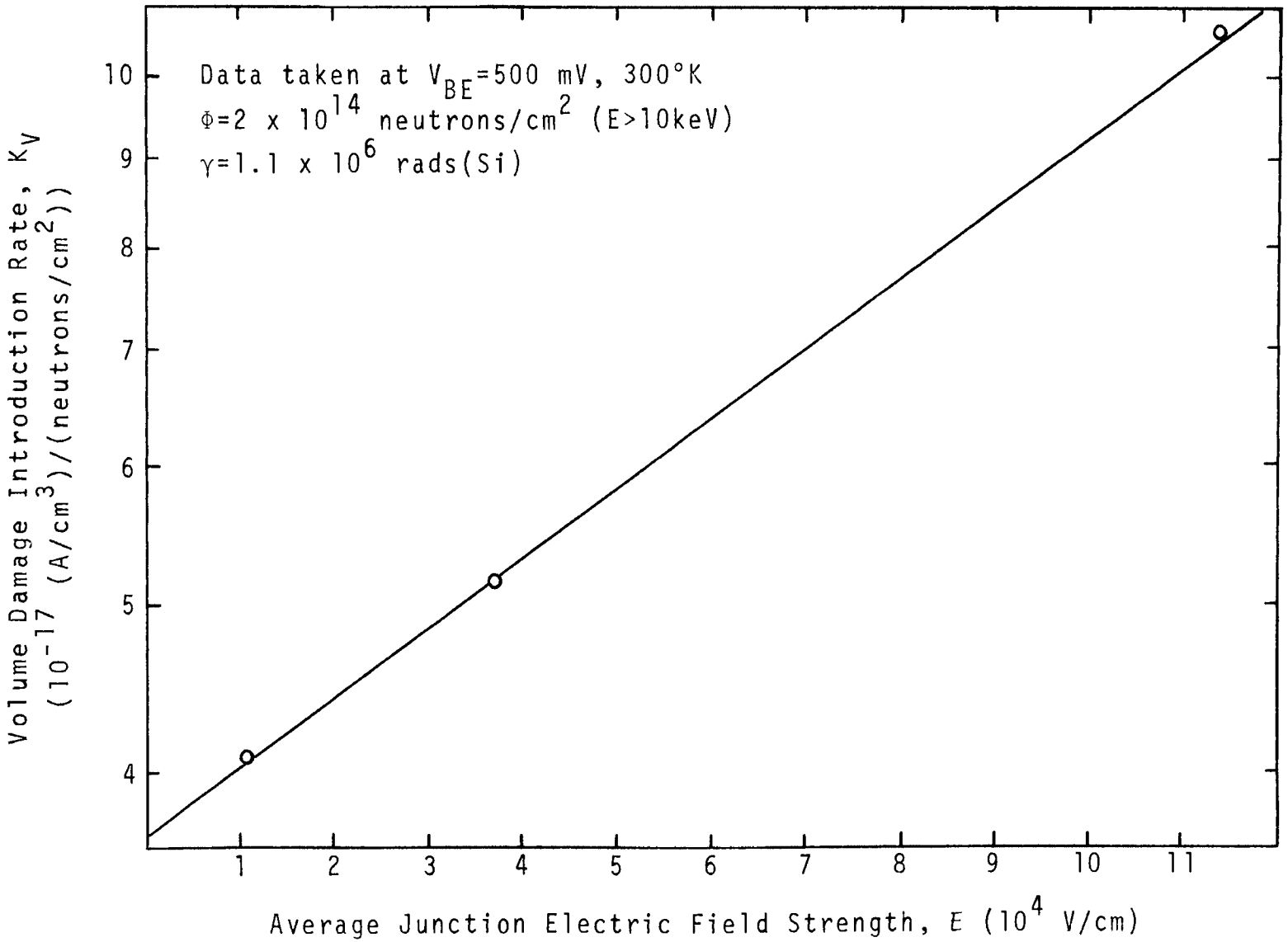

Figure 1b. The volume damage introduction rate versus the average junction electric field strength for matched Motorola 2N914 transistors.

III. CONSIDERATIONS IN THE DETERMINATION OF THE NEUTRON FLUENCE AND JUNCTION ELECTRIC FIELD STRENGTH DEPENDENCE OF THE SPACE-CHARGE REGION VOLUME DAMAGE INTRODUCTION RATE

A. Space-Charge Region Neutron-Induced Base Current Component

The space-charge region volume damage introduction rate is related to the neutron-induced space-charge current component by Equation (1)[6]. This equation indicates that the magnitude of the neutron-induced space-charge component of base current, $\Delta I_{B\Phi}$, the reciprocal slope term, n, and the volume of the emitter-base space-charge region, $A_E \cdot X_m$, must be measured in order to calculate the rate of space-charge volume damage introduction, K_V.

The magnitude of the neutron-induced space-charge component, $\Delta I_{B\Phi}$, can be obtained by removing the "neutral" base region recombination current and separating the gamma-induced surface recombination current from the remaining base current change.

B. Removal of the "Neutral" Base Region Recombination Current

The "neutral" base region recombination current can be removed from the total base current change by using the mathematical model for the base region of graded base devices[4,9]. This model predicts that the neutron-induced "neutral" base region recombination current component is greater than and directly proportional to the observed and

measurable decrease in the collector current.

The ratio of base current increase to collector current decrease was found (for NPN devices) to be[9],

$$R = \frac{\Delta I_{nB}(\Phi)}{\Delta I_{nC}(\Phi)} = \frac{J_{nE}(\Phi) - J_{nC}(\Phi)}{J_{nC}(0) - J_{nC}(\Phi)}$$

$$= \frac{1 + \frac{F(\Phi)}{Z(\Phi)} \coth\left(\frac{W(\Phi)}{Z(\Phi)}\right) - \frac{F(\Phi)}{Z(\Phi)} \exp\left(\frac{W(\Phi)}{F(\Phi)}\right) \operatorname{csch}\left(\frac{W(\Phi)}{Z(\Phi)}\right)}{1 + \coth\left(\frac{W(0)}{F(0)}\right) - \frac{F(\Phi)}{Z(\Phi)} \exp\left(\frac{W(\Phi)}{F(\Phi)}\right) \operatorname{csch}\left(\frac{W(\Phi)}{Z(\Phi)}\right)} \qquad (3)$$

where

ΔI_{nB} = the neutron-induced base current increase (A),

ΔI_{nC} = the neutron-induced collector current decrease and that caused by existing defects (A),

J_{nE} = the injected emitter current density (A/cm^2),

J_{nC} = the fraction of injected emitter current which is collected (A/cm^2),

W = the effective base width (cm),

η = the base region field parameter,

F = the reciprocal electric field parameter [$2W/\eta$ (cm)],

and Z is defined by,

$$\left(\frac{W}{Z}\right)^2 = \left(\frac{W}{F}\right)^2 + \left(\frac{W}{L}\right)^2 = \left(\frac{\eta}{2}\right)^2 + \left(\frac{W}{L}\right)^2 \quad . \qquad (4)$$

$J_{nC}(0)$ is the collector current density in the absence of recombination ($L \to \infty$, $\Phi = 0$). This equation is not directly applicable to the present work since the zero recombination

current is not physically measurable. A logical extension of this work yields,

$$r(\Phi) = \frac{\Delta I_B(\Phi)}{\Delta I_C(\Phi)} = \frac{[I_E(\Phi) - I_C(\Phi)] - [I_E(0) - I_C(0)]}{I_C(0) - I_C(\Phi)}$$

$$= \frac{I_E(\Phi) - I_E(0)}{I_C(0) - I_C(\Phi)} + 1 \qquad (5)$$

where the sign of r is chosen positive. From previous work[9],

$$I_E(\Phi) = A_E \cdot J_{nE}$$

$$= A_E \cdot q \cdot \bar{D}_n(\Phi) \cdot n_e(\Phi)$$

$$\cdot \{1/F(\Phi) + [1/Z(\Phi)] \cdot \coth(W(\Phi)/Z(\Phi))\}$$

$$\cdot \exp(\frac{qV_{BE}}{kT}) \qquad (6)$$

and

$$I_C(\Phi) = A_E \cdot J_{nC}$$

$$= A_E \cdot q \cdot \bar{D}_n(\Phi) \cdot n_e(\Phi) \cdot [1/Z(\Phi)]$$

$$\cdot \exp(W(\Phi)/F(\Phi)) \cdot \operatorname{csch}(W(\Phi)/Z(\Phi))$$

$$\cdot \exp(\frac{qV_{BE}}{kT}). \qquad (7)$$

Thus, $r(\Phi)$ can be written as,

$$r(\Phi) = \{[\frac{1}{F(\Phi)} + \frac{1}{Z(\Phi)} \cdot \coth(\frac{W(\Phi)}{Z(\Phi)})]$$

$$- [\frac{1}{F(0)} + \frac{1}{Z(0)} \cdot \coth(\frac{W(0)}{Z(0)})]\}$$

$$\div \{[\frac{1}{Z(0)} \cdot \exp(\frac{W(0)}{F(0)}) \cdot \operatorname{csch}(\frac{W(0)}{Z(0)})]$$

$$- [\frac{1}{Z(\Phi)} \cdot \exp(\frac{W(\Phi)}{F(\Phi)}) \cdot \operatorname{csch}(\frac{W(\Phi)}{Z(\Phi)})]\} + 1, \qquad (8)$$

which can be rewritten by multiplying and dividing by W as,

$$r(\Phi) = \{[\frac{\eta(\Phi)}{2} + \frac{W}{Z(\Phi)} \cdot \coth(\frac{W}{Z(\Phi)})]$$

$$- [\frac{\eta(0)}{2} + \frac{W}{Z(0)} \cdot \coth(\frac{W}{Z(0)})]\}$$

$$\div \{[\frac{W}{Z(0)} \cdot \exp(\frac{\eta(0)}{2}) \cdot \operatorname{csch}(\frac{W}{Z(0)})]$$

$$- [\frac{W}{Z(\Phi)} \cdot \exp(\frac{\eta(\Phi)}{2} \cdot \operatorname{csch}(\frac{W}{Z(\Phi)})]\} + 1, \qquad (9)$$

where the relationships

$$\frac{1}{F} = \frac{\eta}{2W} \qquad (10)$$

and

$$W(\Phi) \simeq W(0) \simeq W$$

have been used.

C. Separation of the Gamma-Induced Surface Recombination Current

It is necessary to separate the gamma-induced surface recombination-generation current from the total base current changes in order to study the bulk effects. This could have been done using an expression[10,11] relating the gamma-induced surface recombination current to the initial base current, I_{BS}, the electric field strength present during exposure, E, and the ionizing radiation dose, γ. The expression,

$$\Delta I_{B\gamma}(V_{BE},E,\gamma) = I_{BS}(V_{BE}) \cdot f(E,\gamma).$$

$$= I_{BS}(V_{BE}) \cdot \alpha \cdot E^{\beta}$$

$$\cdot [(1 - \exp([1 + E/E_o]\gamma/\gamma_o)] \qquad (11)$$

where

$\alpha = 0.17$,

$\beta = 0.435$,

$E_o = 8.9 \times 10^4$ V/cm, and

$\gamma_o = 7.9 \times 10^5$ rad(Si)

was determined by fitting experimental data[10]. Equation (10) was only shown to be applicable to special matched devices[10]. However, it does suggest an experimental technique for separating this component by noting that the gamma-induced surface component saturates at high doses (about 10^6 rads(Si)).

The total base current change has been shown to be

dominated over a wide current/injection range by the neutron-induced space-charge region recombination current discussed in Section A, the neutron-induced "neutral" base recombination current discussed in Section E, and the gamma-induced surface recombination current discussed in this Section. The resultant equation for this range can be written as,

$$\Delta I_{Btot}(V_{BE},E,\Phi,\gamma) = \Delta I_{B\Phi}(V_{BE},E,\Phi) + \Delta I_{B\gamma}(V_{BE},E,\gamma) + r(\Phi) \cdot \Delta I_{C}(V_{BE},\Phi) \quad . \tag{12}$$

Using Equation (1), Equation (12) may be rewritten as,

$$\Delta I_{Btot}(V_{BE},E,\Phi,\gamma) - r(\Phi) \cdot \Delta I_{C}(V_{BE},\Phi) = \Delta I_{B\gamma}(V_{BE},E,\gamma) + K_V \cdot X_m \cdot \Phi \cdot A_E \cdot \exp(qV_{BE}/nkT) \tag{13}$$

where all terms are as previously defined.

D. Reciprocal Slope Term

The reciprocal slope term, n, has been measured for 2N914 transistors and was found to vary, for 0.15 eV $< (E_i - E_R) <$ 0.35 eV and $V_{BE} <$ 0.75, as[12,13],

$$\frac{1}{n} = 0.4107 + \frac{kT}{q} \cdot \frac{1.21 \times 10^{-3}}{V_Z(V_{BE},\Phi) - V_{BE}} + \frac{kT}{q} \cdot \frac{2.948}{E_i - E_R} + 6.34 \times 10^{-3} \cdot \ln\left(\left[\frac{\sigma_p}{\sigma_n}\right]^{1/2} + \left[\frac{\sigma_n}{\sigma_p}\right]^{1/2}\right) \tag{14}$$

where

V_Z = diffusion potential (V),

E_i = the intrinsic Fermi energy (0.55 eV),

E_R = the defect energy (0.235 eV),

σ_n = electron capture cross-section (8.1×10^{-16} cm^{-2}),

σ_p = hole capture cross-section (1.8×10^{-16} cm^{-2})

and k, T, and q have the standard meanings, respectively, of Boltzman constant, absolute temperature and electronic charge. The parameters in Equation (14) have been previously measured[12] for 2N914 transistors and were used to evaluate n.

E. Calculation of the Diffusion Potential (V_Z)

The junction capacitance can be modeled by an equation of the form,

$$C_T(V_{BE},\Phi) = \frac{R(V_{BE},\Phi)}{[V_Z(V_{BE},\Phi) + V_{BE}]^{x_n(V_{BE},\Phi)}} , \qquad (15)$$

where

C_T = the junction capacitance (F),

R = a parameter of fit related to the junction area, profile, and material,

V_Z = the junction diffusion potential (V), and

x_n = a parameter of fit related to the profile which varies from 1/2 for a step junction to 1/3 for a linearly graded junction.

The theoretical dependence of R, V_Z, and x_n on V_{BE} has

been determined[14] for non-irradiated 2N914 transistors. The diffusion potential was found to vary approximately logarithmically with the total junction potential, $V_Z + V_{BE}$, and x_n was found to vary approximately linearly with the applied voltage, V_{BE}. The results for x_n are tabulated in Table 1.

V_{BE}	x_n	V_{BE}	x_n	V_{BE}	x_n
0.49	0.3392	-0.04	0.3452	-2.25	0.3617
0.45	0.3398	-0.40	0.3479	-2.50	0.3636
0.40	0.3412	-1.01	0.3533	-4.40	0.3788
0.04	0.3440	-1.15	0.3555	-4.80	0.3806

Table 1. x_n as a function of voltage for the 2N914 transistor code[14].

Using these results for x_n, the pre-irradiation value of the diffusion potential, V_Z, can be approximated, assuming V_Z, and x_n constant over a small range of V_{BE}, by

$$V_Z(V) = \{[V + \Delta V] \cdot [C_T(V + \Delta V)]^{1/x_n(V)} - [V - \Delta V] \cdot [C_T(V - \Delta V)]^{1/x_n(V)}\} \div \{[C_T(V - \Delta V)]^{1/x_n(V)} - [C_T(V + \Delta V)]^{1/x_n(V)}\} \quad (16)$$

If the variation of x_n with neutron fluence was known, then Equation (16) could be used to calculate the diffusion potential for each fluence. However, this dependence has not been obtained. Therefore, the neutron fleunce depen-

dence of the diffusion potential will be approximated using[6]

$$V_Z(V_{BE},\Phi) = V_Z(V_{BE},0) - \frac{kT}{q} K_1 \Phi \qquad (17)$$

where K_1 was found to be 1.27×10^{-16} cm^2/neutron for 2N914 transistors.

F. Calculation of the Depletion Layer Width and the Average Junction Electric Field

The depletion layer width can be calculated from the junction capacitance as[8],

$$X_m(V_{BE},\Phi) = \frac{A_E \cdot \varepsilon \cdot \varepsilon_o}{C_T(V_{BE},\Phi)} , \qquad (18)$$

where

C_T = the junction capacitance (F),

X_m = the depletion layer width (cm),

ε_o = the permittivity of free space (8.85×10^{-14} F/cm), and

ε = the relative permittivity of the semiconductor material (11.8 for silicon).

The average pre-irradiation electric field strength is calculated as,

$$E = \frac{V_Z(V_{BE},0) + V_{BE}}{X_m(V_{BE},0)} . \qquad (19)$$

IV. EXPERIMENTAL TECHNIQUE

A. Pre-irradiation Treatment and Irradiation Techniques

The devices used in this work were annealed for 12 hours at 250°C to remove internal stresses produced during manufacturing. All irradiations were carried out in the University of Missouri-Rolla Research Reactor[12]. The devices were irradiated simultaneously to insure similar radiation conditions. The neutron fluence was monitored using nickel foil dosimetry and the corresponding gamma dose calculated using a gamma-to-neutron ratio of 1.14×10^{-8} rads(Si)/(neutrons/cm^2)[10].

After irradiation, the devices were stored at room temperature for eight hours to allow any transient annealing to be completed. At all other times the devices were stored in liquid nitrogen to prevent long term room temperature annealing. This precaution was necessary since the irradiations were carried out over a period of 3 months. Since the quenching from room temperature to liquid nitrogen temperature and subsequent warming could conceivably introduce thermal stress, an experiment was performed on several similar devices which were alternately quenched to liquid nitrogen temperature and then heated to room temperature. These devices exhibited no measurable change in their electrical characteristics. Thus, thermally-induced stresses were assumed to be negligible.

B. Measurement and Treatment of Current/Voltage (I/V) Data

The base and collector currents were measured, before irradiation and after each subsequent irradiation, over a range of base-to-emitter voltages of 100 to 800 millivolts using the Automatic Data Acquisition System of the Electronics Research Laboratory of the Materials Research Center[12].

The results of the calculation of the ratio of base current increase to collector current decrease are tabulated in Table 2. The ratio r is seen to decrease slowly with neutron fluence as shown in Figure 2. The magnitude of r is seen to be 4.25 to 4.75 and not one as would have been previously expected. This can be understood by considering the carrier distribution in the base for a constant injection level:

Fluence	r(Φ)	Fluence	r(Φ)	Fluence	r(Φ)
2.7×10^{12}	4.803	3.5×10^{13}	4.795	2.8×10^{14}	4.725
5.3×10^{12}	4.798	4.3×10^{13}	4.793	3.6×10^{14}	4.702
7.5×10^{12}	4.801	5.2×10^{13}	4.789	4.6×10^{14}	4.673
9.9×10^{12}	4.804	6.0×10^{13}	4.788	5.7×10^{14}	4.648
1.4×10^{13}	4.802	7.7×10^{13}	4.783	6.8×10^{14}	4.622
1.6×10^{13}	4.800	9.5×10^{13}	4.778	7.7×10^{14}	4.599
2.0×10^{13}	4.799	1.4×10^{14}	4.764	8.8×10^{14}	4.573
2.4×10^{13}	4.799	1.9×10^{14}	4.750	1.0×10^{15}	4.548
3.1×10^{13}	4.797	2.4×10^{14}	4.737	1.1×10^{15}	4.524

Table 2. The ratio of base current increase to collector current decrease as a function of neutron fluence.

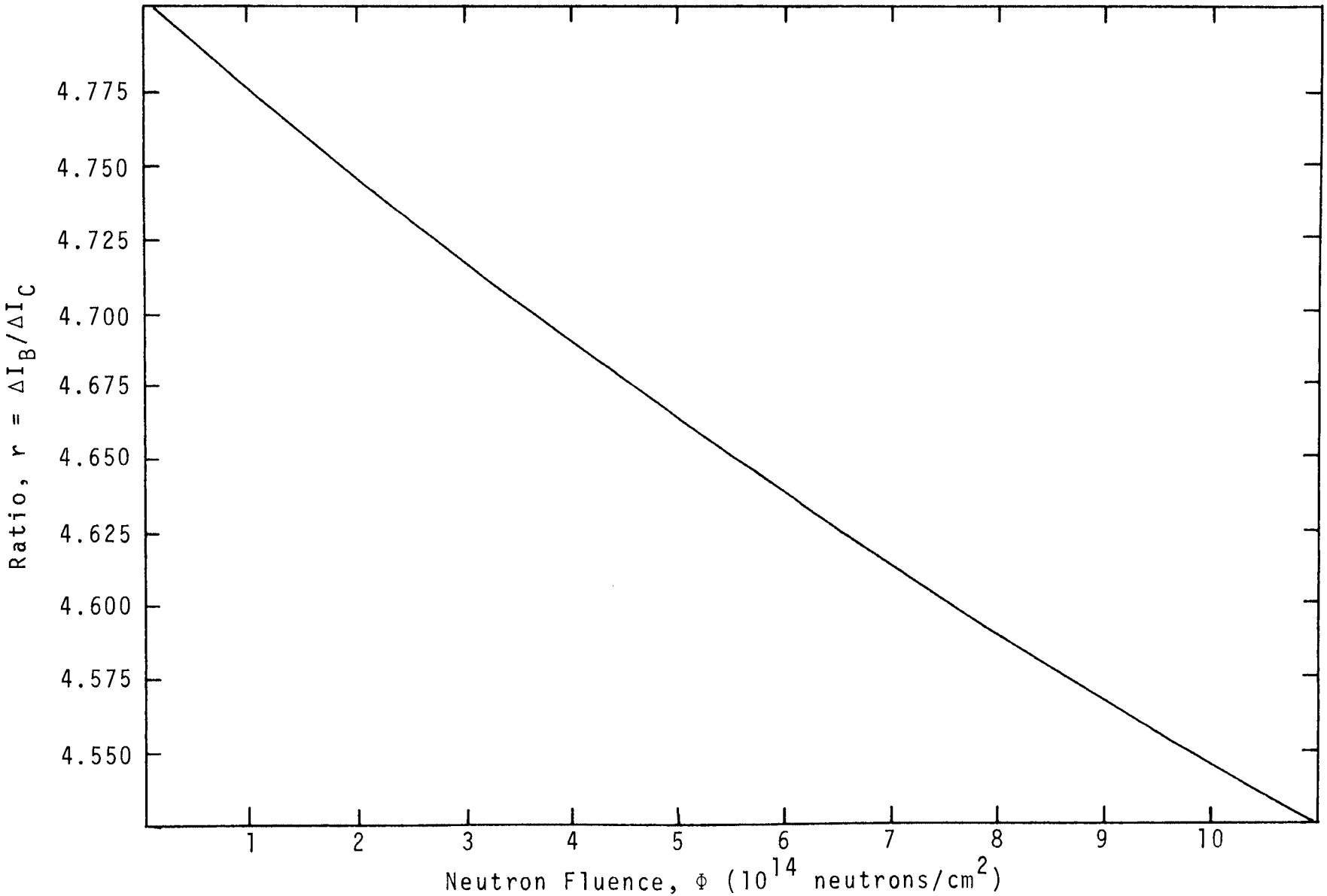

Figure 2. The ratio of base current increase to collector current decrease as a function of neutron fluence for the special devices.

> "Neutron-induced recombination reduces the excess minority carrier density everywhere in the base below the one which is present in the case of little or no recombination. The excess minority carrier concentrations at the emitter and collector side of the active base region are held fixed by their respective base voltages. Thus, the neutron-induced recombination forces the excess carrier gradient to increase at the emitter side and to decrease at the collector side. Since current is proportional to both the excess carrier concentration and gradient, this corresponds to an increase in emitted current and a decrease in collected current. The base current increase is the sum of the absolute magnitudes of the two and is consequently larger than either one."[9]

The device parameters used in calculating the ratio of base current increase to collector current decrease are listed in Table 3.

The collector current decrease was calculated using[4]

$$\Delta I_C(V_{BE},\Phi) = I_{Co}(V_{BE}) \cdot K_2 \cdot \Phi \quad , \tag{20}$$

where

ΔI_C = the collector current decrease at the voltage and fluence of interest (A),

I_{Co} = the pre-irradiation collector current at the same voltage (A),

K_2 = damage constant for the collector current of these devices (2.5×10^{-16} cm^2/neutron)[4]

C. Measurement and Treatment of Capacitance/Voltage (C/V) Data

The emitter-base junction capacitance needed for this work was measured on the Capacitance/Voltage Measurement

PARAMETER	UNITS	SPECIAL DEVICES	2N914
N_{oE}-emitter diffusion surface concentration	cm^{-3}	$\simeq 2 \times 10^{21}$	$\simeq 2 \times 10^{21}$
N_{oB}-base diffusion surface concentration	cm^{-3}	$\simeq 5 \times 10^{19}$	$\simeq 5 \times 10^{19}$
N_{BC}-collector background concentration	cm^{-3}	$\simeq 5 \times 10^{15}$	$\simeq 5 \times 10^{15}$
x_{je}-emitter junction depth	cm	$\simeq 2 \times 10^{-4}$	$\simeq 2 \times 10^{-4}$
x_{jc}-collector junction depth	cm	$\simeq 3 \times 10^{-4}$	$\simeq 3 \times 10^{-4}$
η-base field parameter		2.1	2.1
W-base width	cm	9.0×10^{-5}	6.0×10^{-5}
K_1-diffusion potential damage constant	cm^2/neutron	1.27×10^{-16}	1.27×10^{-16}
K_2-collector current damage constant	cm^2/neutron	2.5×10^{-16}	3.5×10^{-16}
τ_n-minority carrier lifetime	s	3.0×10^{-8}	1.2×10^{-8}
K_τ-lifetime damage constant	cm^2/neutron-s	2.0×10^{-6}	2.0×10^{-6}
μ_n-minority carrier mobility	cm^2/V-s	4.6×10^{2}	4.4×10^{2}
K_μ-mobility damage constant	cm^2/neutron	7.0×10^{-16}	7.0×10^{-16}
ρ_s-base sheet resistivity	ohms/□	2.25×10^{3}	4.0×10^{3}
R_{ex}-base external resistance	ohms	9.0	12.8
A_E-emitter area	cm^2	7.85×10^{-5}	7.85×10^{-5}

Table 3. Parameters for the test devices[9].

System of the Electronics Research Laboratory of the Materials Research Center[12]. The measured capacitance was corrected for the emitter-base junction header capacitance and the device stray capacitance. This correction was determined to be 0.3 pF using destructive testing methods on several similar devices.

The capacitance as corrected consists of the junction capacitance and the base region diffusion capacitance. The diffusion capacitance is negligible for reverse bias, but not for forward bias. The tabulated values of x_n (Table 1) confirms that the junction in the forward bias region is approximately a linearly graded junction. Combining Equation (15) and (17) the capacitance at any forward bias, V_{BE}, and fluence, Φ, can be approximated by

$$C(V_{BE},\Phi) = C(0,\Phi) \cdot \left\{\frac{V_Z(0,0) - \frac{kT}{q} K_1 \cdot \Phi}{V_Z(V_{BE},0) - \frac{kT}{q} K_1 \cdot \Phi + V_{BE}}\right\}^{1/3} \quad (21)$$

The pre-irradiation diffusion potential was calculated using Equation (16). The average value, obtained from four data points spaced at 0.02 V increments about the bias of interest, was used for V_Z at zero and reverse bias. The diffusion potential for forward biases was obtained by extrapolating values obtained at zero and one volt reverse bias to the forward bias of interest. The neutron fluence dependence of V_Z was then introduced through Equation (17).

D. Data Presentation

To obtain the exact electric field strength dependence and to check for a neutron fluence dependence of K_V, the techniques of Section II were applied to six special devices manufactured by Texas Instruments to meet the same transistor code as the 2N914 except without the gold doping. These were irradiated at room temperature to a neutron fluence of 10^{15} neutron/cm^2 in 28 irradiation steps. Three of six devices were matched to within ±35% for use in the determination of the field dependence of K_V. Shown in Table 4 are the biases used with these devices during irradiation and the resultant initial average fields. Table 4 also contains several other device-dependent initial values which were used in this work.

In addition to the measurements listed above in Sections B and C, the reverse saturation current for the base and collector were measured approximately every third irradiation and the collector capacitance every irradiation. These data were taken to check for the possibility of the formation of surface channels.

It is of interest to examine the current/voltage characteristics of the three matched devices, one of which was forward biased, one unbiased, and the other reverse biased during irradiation. Current/voltage characteristics for this set of devices prior to irradiation and at a fluence of 10^{15} neutron/cm^2 (E>10keV) are shown in Figure 3. The collector current is found to be invariant with the emitter-

Parameter	Condition	Units	Device					
			15	18	24	25	45	79
I_B-Base Current	V_{BE}=0.5 V	nA	631.5	140.3	112.5	67.27	77.10	132.8
I_C-Collector Current	V_{BE}=0.5 V	μA	3.716	2.034	5.244	1.152	5.612	5.277
h_{FE}-Common Emitter Current Gain	V_{BE}=0.5 V		5.885	14.50	46.63	17.12	72.79	39.73
C_T-Emitter Junction Capacitance	V_{BE}=0.0 V	pf	6.19	6.90	5.89	7.77	5.81	5.89
V_Z-Diffusion Potential	V_{BE}=0.0 V	V	0.76	0.71	0.73	0.72	0.76	0.73
V^*_{BE}-Base-Emitter Bias, During Irradiation		V	0.6	-1.07	0.5	-4.5	0.0	-2.4
V_Z-Diffusion Potential During Irradiation	$V_{BE}=V^*_{BE}$	V	0.70	0.84	0.71	0.95	0.76	0.83
$\mathcal{E}$-Junction Field, During Irradiation	$V_{BE}=V^*_{BE}$	kV/cm	14.6	117.	22.4	246.	52.8	172.
I_{BR}-Reverse Saturation Base Current	V_{BE}=-5 V	pA	67.68	38.13	37.79	451.6	32.85	23.65

Table 4. Device initial parameters.

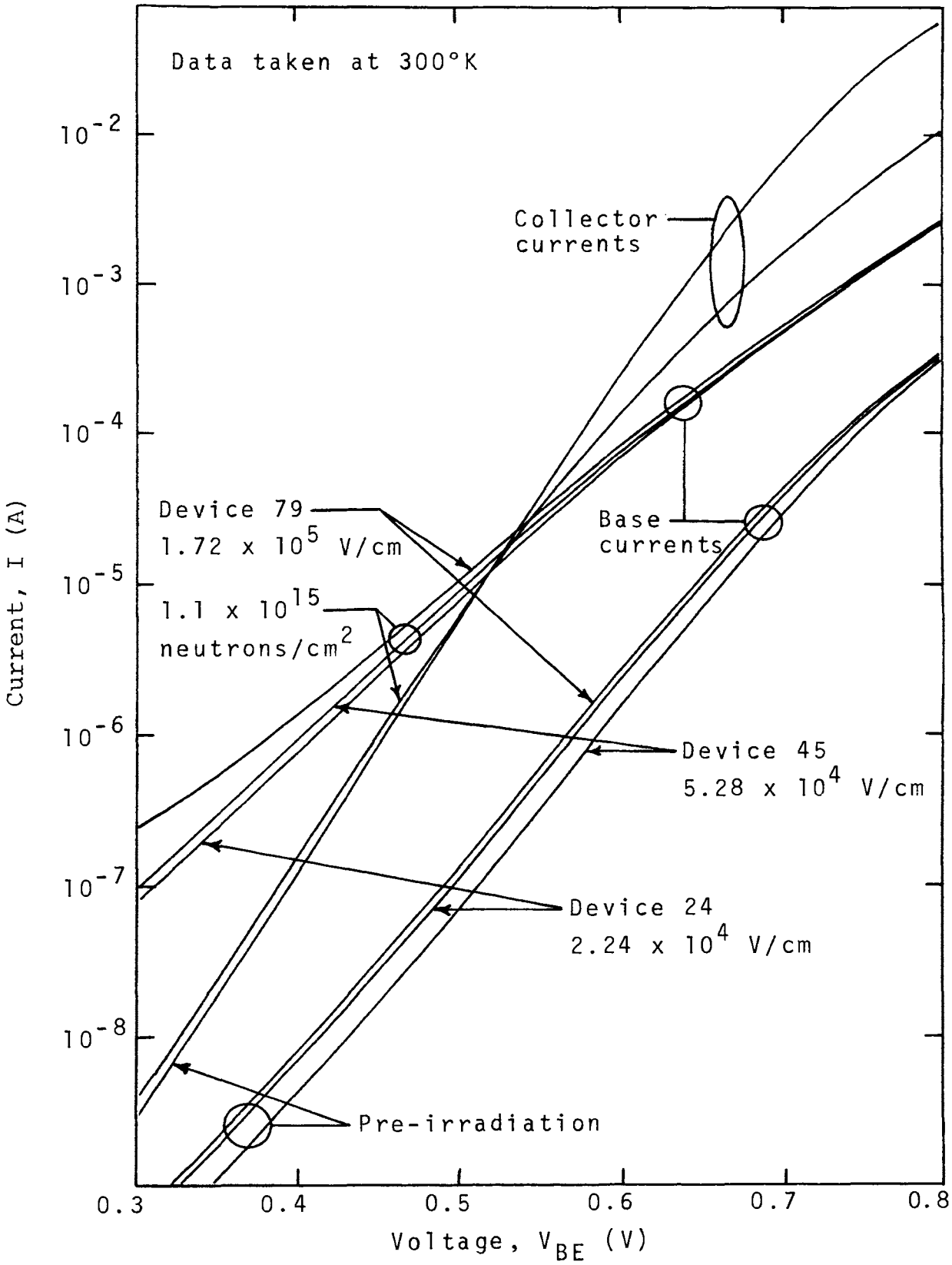

Figure 3. Current versus voltage for specially fabricated Texas Instruments devices with junction electric field strength during irradiation as a parameter.

base junction field present during irradiation. This would not be expected, since the collector current would be affected by recombination in the "neutral" base region, which is reduced by increasing reverse emitter bias. The absence of any observable difference may indicate that the defect formed in the "neutral" base when it is not neutral (i.e., in the region where the emitter base junction spreads into the base with a reverse bias during irradiation) may be indistinguishable from the defect formed in the "neutral" base when it is neutral (i.e., the same region when irradiated with zero or forward bias). More likely, however, it simply indicates that the volume affected (8 percent) is too small for any effect to be observed.

The base current depicted in Figure 3 is observed to vary with the junction electric field strength existing during irradiation. This variation can be seen, from the slope of the base current at the intermediate current levels, to be dominated by changes in the neutron-induced space-charge recombination current component, rather than by surface effects. It should be noted here that the data in Figure 3 are for a relatively high neutron fluence, and surface effects would not be detected easily at this fluence by a "slope change" since the gamma-induced surface effects begin to saturate at 1-2 x 10^5 rads(Si) (corresponding to 1-2 x 10^{13} neutrons/cm^2) and are nearly completely saturated at 10^6 rads(Si) (corresponding to 10^{14} neutrons/cm^2)[10,11]. The recombination in the emitter base space-charge region is

observed from the data in Figure 3 to increase with increasing electric field strength, indicating that the severity of neutron-induced recombination at higher fluences in the space-charge region of an operating device is governed by the magnitude of the electric field present in the junction during irradiation.

The pre-irradiation diffusion potential, V_Z, and the depletion layer width, X_m, were calculated from the capacitance/voltage data for the bias during irradiation using the techniques outlined in Section II E. These values are necessary in order to determine the average junction electric field strength. In addition, the depletion layer width was calculated for a V_{BE} of 500 mV forward measurement bias for the calculation of the S-CRV damage introduction rate.

It was found that the S-CRV damage introduction rate, K_V, could be obtained by plotting the parameter, K_{tot}, defined as,

$$K_{tot} = \frac{\Delta I_{Btot}(V_{BE},E,\Phi,\gamma) - r(\Phi) \cdot \Delta I_C(V_{BE},\Phi)}{\Phi \cdot X_m \cdot A_E \cdot \exp(qV/nkT)} \qquad (22)$$

versus the neutron fluence. On comparing Equation (22) with Equation (12) and (13), K_{tot} can be s-en to be a total damage introduction rate attributable to the combined effect of neutrons and gamma. Figure 4, which is a typical plot of K_{tot} versus Φ, shows two regions which may be separated from each other by extrapolating backward the linear region at high fluences/doses. The curve from low fluences

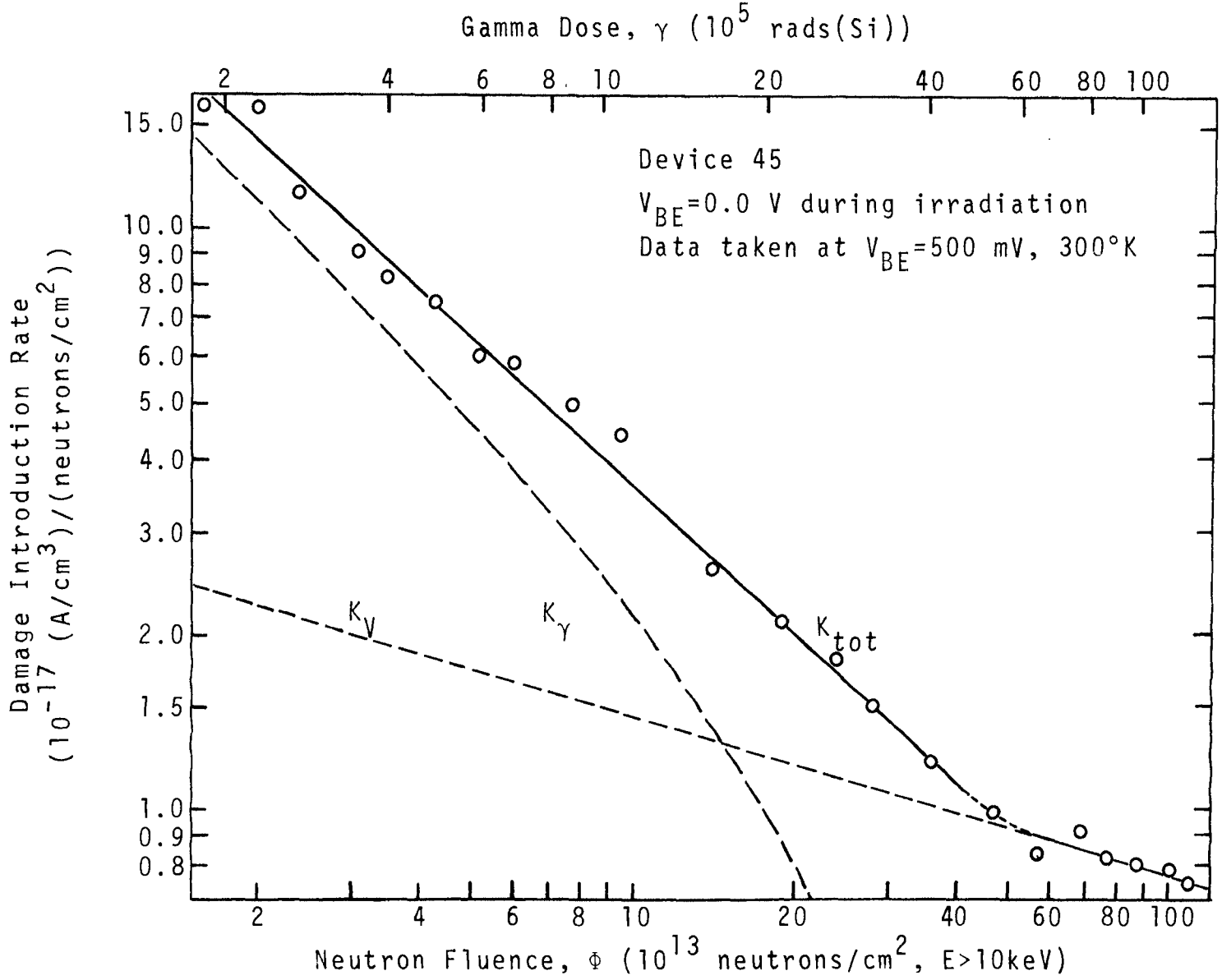

Figure 4. The damage introduction rate versus the neutron fluence.

to about 5 x 10^{14} neutrons/cm^2 is a result of the combined effects of neutrons and gamma dose. The gamma dose effect saturates at about 10^{14} neutrons/cm^2; thus the curve from 5 x 10^{14} neutrons/cm^2 to 10^{15} neutrons/cm^2 is dominated solely by neutron effects. The separation of the K_{tot} curve into K_V and K_γ is also indicated in Figure 4 along with the backward extrapolation.

The data in that portion of Figure 4 attributed to gamma-induced surface effects has also been normalized with respect to the space-charge volume parameters (i.e., volume, neutron fluence, and the exponential term). If the gamma dose and device parameter dependencies of the gamma-induced surface effect were desired the data would have to be re-normalized to surface parameters (i.e., surface area and gamma dose). Re-normalization is not needed in this work since we are interested primarily in neutron effects. The total damage introduction rate as calculated from Equation (22) for six special devices is tabulated in Table 5. Plotted in Figure 5 with the average electric field strength as a parameter are the measured S-CRV damage introduction rate versus the neutron fluence. The S-CRV damage introduction rate, K_V, was found to follow a function of the form[10],

$$K_V = K_{Vo}\left[\frac{\Phi}{\Phi_o}\right]^{-m(E)} \qquad (23)$$

where

Neutron Fluence (Φ)	K_{tot} (10^{-17} (A/cm^3)/(neutrons/cm^2))					
	Matched Devices			Unmatched Devices		
	No. 24	No. 45	No. 79	No. 15	No. 18	No. 25
9.9×10^{12}	2.37	3.04	60.90	33.09	8.16	18.60
1.4×10^{13}	2.41	5.07	48.24	25.99	9.22	14.75
1.6×10^{13}	3.53	16.39	46.53	26.98	11.22	18.22
2.0×10^{13}	3.42	16.00	37.30	23.54	10.35	15.83
2.4×10^{13}	3.13	11.54	30.62	19.84	9.89	11.85
3.1×10^{13}	3.01	9.06	25.20	17.20	9.17	10.13
3.5×10^{13}	2.77	8.28	22.11	15.50	8.57	8.61
4.3×10^{13}	2.80	7.51	18.58	14.00	7.98	9.16
5.2×10^{13}	2.66	6.04	14.58	11.30	6.82	8.97
6.0×10^{13}	2.78	5.94	13.60	10.89	6.68	7.05
7.7×10^{13}	2.74	4.95	11.09	9.36	5.95	6.40
9.5×10^{13}	2.59	4.39	9.39	8.38	5.46	5.35
1.4×10^{14}	2.20	2.56	6.21	6.50	4.37	5.16
1.9×10^{14}	1.98	2.08	4.97	5.18	3.68	4.43
2.4×10^{14}	1.47	1.79	3.93	4.15	3.13	3.71
2.8×10^{14}	1.24	1.49	3.48	3.64	2.90	3.36
3.6×10^{14}	0.92	1.17	2.77	2.89	2.54	2.43
4.7×10^{14}	0.91	0.98	2.30	2.59	2.26	2.44
5.7×10^{14}	0.71	0.83	1.98	2.26	2.13	1.92
6.8×10^{14}	0.79	0.91	1.96	2.23	2.07	2.30
7.7×10^{14}	0.68	0.82	1.76	2.07	1.99	1.93
8.8×10^{14}	0.71	0.80	1.64	2.05	1.95	1.82
1.0×10^{15}	0.64	0.78	1.56	2.07	1.95	1.98
1.1×10^{15}	0.64	0.74	1.42	1.84	1.85	2.00

Table 5. The damage introduction rate versus neutron fluence at V_{BE} equal to 500 mV.

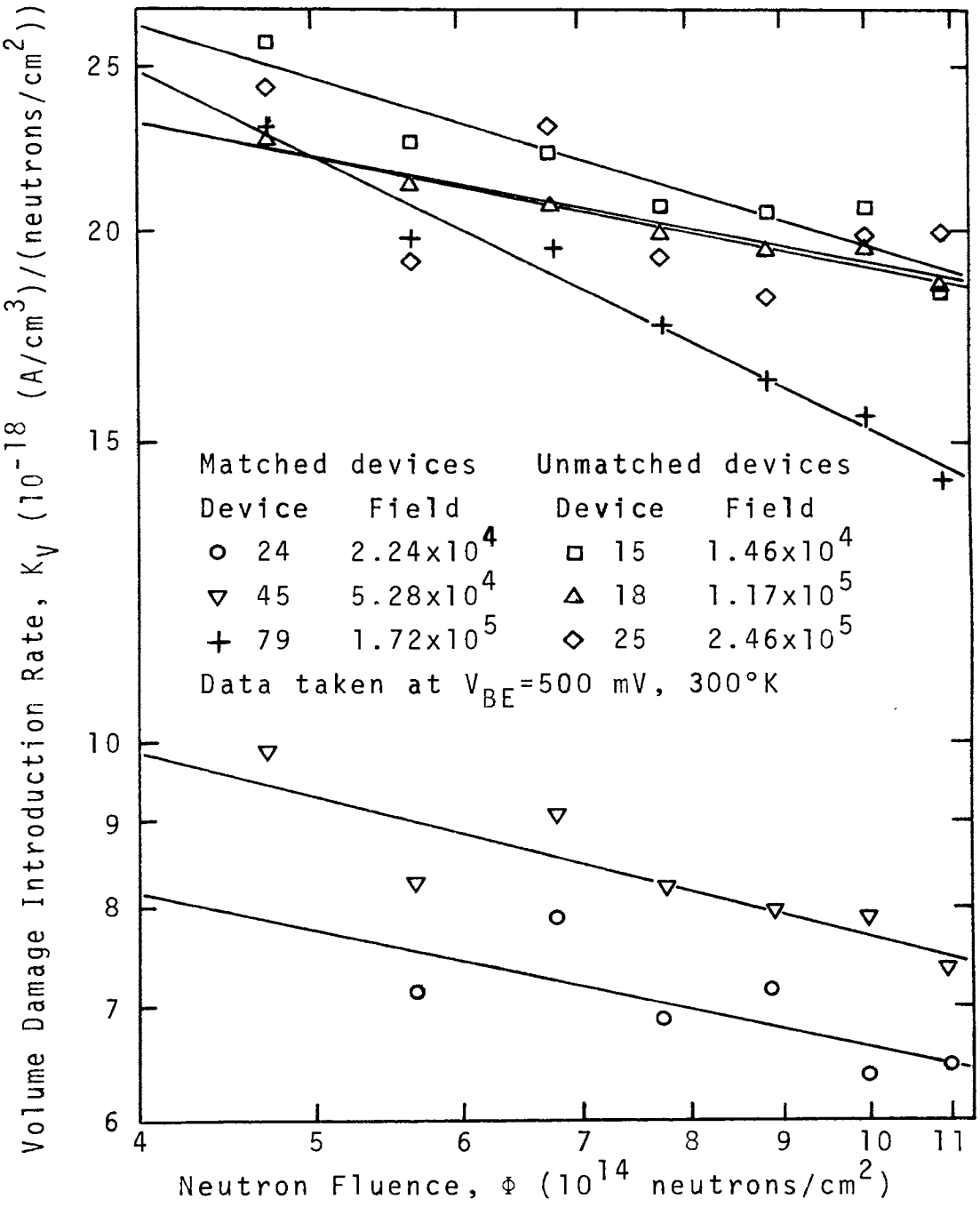

Figure 5. The volume damage introduction rate versus neutron fluence with the average junction electric field strength during irradiation as a parameter.

$K_{Vo} = 2.28 \times 10^{-17}$ $(A/cm^3)/(neutrons/cm^2)$,

$\Phi_o = 1.98 \times 10^{14}$ $(neutrons/cm^2)$, and

$m(E)$ = the slope.

For the three matched devices, Figure 5 shows the previously mentioned field dependence; the higher the electric field the larger is the volume damage introduction rate, K_V. Equation (23) shows that the electric field strength dependence enters through the power term, $m(E)$. The results of a linear least squares fit of the data from 5×10^{14} to 1.1×10^{15} neutrons/cm^2 are tabulated is Table 6, where $m(E)$ is the quantity of principal interest. The quantity $m(E)$ is plotted in Figure 6, versus the average junction

Device	Slope(m)	Intercept	Least Squares Standard Error
15	0.33	-27.16	0.07×10^{-17}
18	0.21	-31.15	0.02×10^{-17}
24	0.23	-31.72	0.04×10^{-17}
25	0.20	-31.50	0.17×10^{-17}
45	0.31	-28.18	0.07×10^{-17}
79	0.53	-20.48	0.04×10^{-17}

Table 6. Results of least squares fit of K_V versus Φ.

electric field, E. For the three matched devices $m(E)$ is seen to vary with the average field as,

$$m = \left[\frac{E}{E_o}\right]^s \tag{24}$$

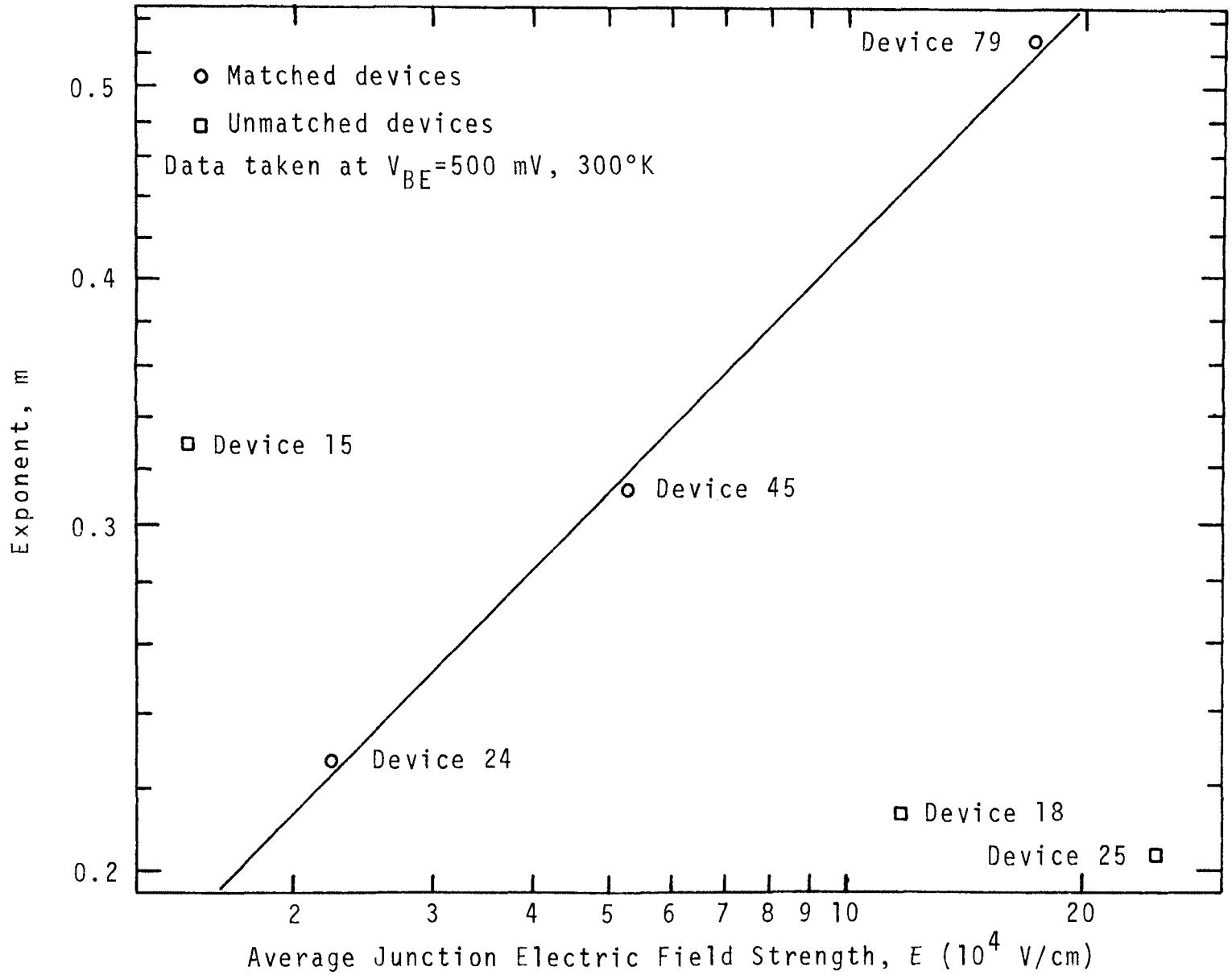

Figure 6. The exponent, m, versus the average junction electric field strength.

where

$E_o = 3.05 \times 10^6$ (V/cm)

$s = 0.218$.

The departure from this behavior for the three unmatched devices is not understood. Device 15, irradiated at 0.6 volts forward bias, should have realized the least damage, but, in fact, showed about the most. Capacitance and leakage current measurements indicate the formation of a surface channel on this device which could account for the large deviation.

Device 25, which was most heavily reverse biased, showed less damage than was expected. Pre-irradiation data indicated the possibility of a much poorer surface condition prior to irradiation, which could account for the apparent lower neutron damage. Device 18,which was also reverse biased, showed less damage than was expected. No explanation for the behavior of this particular unmatched device could be derived from the measurements made on its electrical characteristics.

Equation (20) was used in this work to calculate ΔI_C and good agreement was found with measured values for the three unmatched devices. However, the three matched devices behaved differently than predicted. The collector currents showed only a slight decrease up to about 7×10^{14} neutrons/cm^2 and then increased slightly above their initial value. This behavior is not understood, but since all three matched devices behaved similarly their correlation is still

considered to be valid.

E. Error Analysis

The basic equation one must examine to determine the possible error in the calculation of K_{tot} is Equation (22). On assigning the appropriate error limits in Equation (22) one can write,

$$K_{tot} = \{\Delta I_{Btot} \cdot [1 \pm 0.01] - r(\Phi) \cdot \Delta I_C \cdot [1 \pm 0.24]\}$$

$$\div \{\Phi \cdot [1 \pm 0.2] \cdot X_m \cdot [1 \pm 0.01] \cdot A_E$$

$$\cdot \exp(qV \cdot [1 \pm 0.01]/nkT[1 \pm 0.5/T])\} \qquad (25)$$

where the potential error in ΔI_C was determined from Equation (20) as,

$$\Delta I_C = I_{Co} \cdot [1 \pm 0.01] \cdot K_2 \cdot [1 \pm 0.03] \cdot \Phi \cdot [1 \pm 0.2] \qquad (26)$$

and the error in the area, A_E was considered negligible. The possible error in K_{tot} will depend on the relative magnitude of the quantities, I_B, I_{Co}, X_m, and Φ. A numerical analysis of the data was made for all devices using the worst case conditions for the variables in Equation (25). The results of the analysis for Device 25, which showed the largest potential percentage error, are tabulated in Table 7 and plotted in Figure 7 with error flags. For this device, the potential percentage error is seen to remain fairly constant between 23 and 28 percent. It should be noted that

Neutron Fluence (Φ)	K_{tot} (A/cm^3) ÷ (neutrons/cm^2)	Percentage Error +	Percentage Error -	Neutron Fluence (Φ)	K_{tot} (A/cm^3) ÷ (neutrons/cm^2)	Percentage Error +	Percentage Error -
9.9×10^{12}	1.86×10^{-16}	27.4	17.9	1.4×10^{14}	5.16×10^{-17}	26.2	17.1
1.4×10^{13}	1.48×10^{-16}	27.4	17.9	1.9×10^{14}	4.43×10^{-17}	25.9	16.9
1.6×10^{13}	1.82×10^{-16}	27.4	17.9	2.4×10^{14}	3.71×10^{-17}	25.6	16.7
2.0×10^{13}	1.58×10^{-16}	27.3	17.8	2.8×10^{14}	3.36×10^{-17}	25.3	16.6
2.4×10^{13}	1.19×10^{-16}	27.0	17.6	3.6×10^{14}	2.43×10^{-17}	24.4	16.0
3.1×10^{13}	1.01×10^{-16}	27.0	17.6	4.7×10^{14}	2.44×10^{-17}	24.4	16.0
3.5×10^{13}	8.61×10^{-17}	26.8	17.5	5.7×10^{14}	1.92×10^{-17}	23.5	15.4
4.3×10^{13}	9.16×10^{-17}	26.9	17.6	6.8×10^{14}	2.30×10^{-17}	23.5	15.4
5.2×10^{13}	8.97×10^{-17}	26.9	17.6	7.7×10^{14}	1.93×10^{-17}	23.4	15.3
6.0×10^{13}	7.05×10^{-17}	26.6	17.4	8.8×10^{14}	1.82×10^{-17}	23.1	15.1
7.7×10^{13}	6.40×10^{-17}	26.5	17.3	1.0×10^{15}	1.98×10^{-17}	23.3	15.2
9.5×10^{13}	5.35×10^{-17}	26.2	17.1	1.1×10^{15}	2.00×10^{-17}	23.2	15.2

Table 7. The damage introduction rate for device 25, with percentage error, as a function of neutron fluence.

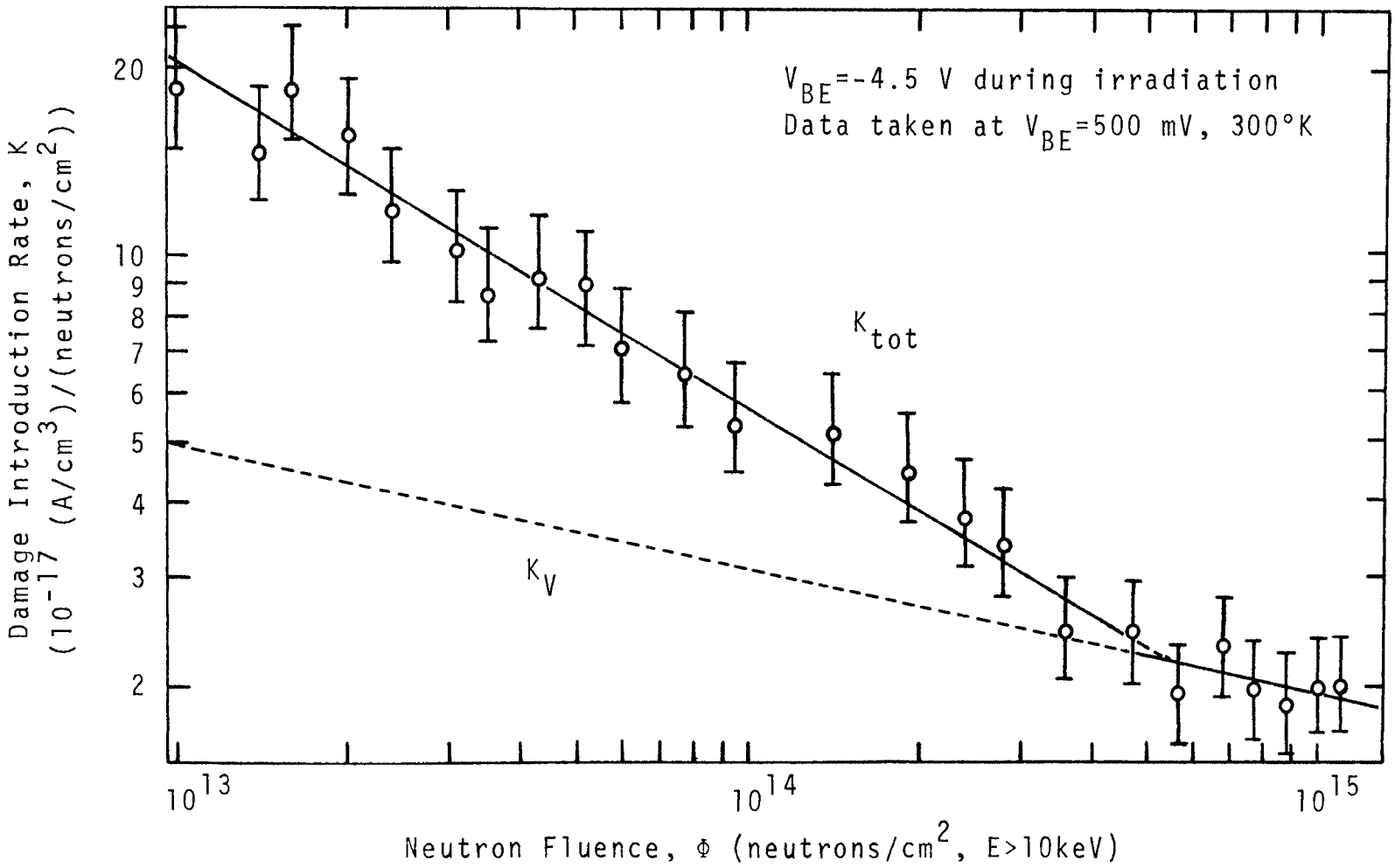

Figure 7. The damage introduction rate versus the neutron fluence for device 25 with error flags.

the absolute error decreases with fluence as a result of the decrease with fluence of K_{tot}.

The potential error in K_V was estimated using the least squares standard error. This potential error was shown in Table 6.

V. SUMMARY AND DISCUSSION

The electric field strength and neutron fluence dependence of the rate of space-charge volume damage introduction was investigated. An experimental technique was developed to facilitate the separation of gamma-induced surface effects from neutron-induced bulk space-charge effects. The results of previous theoretical work[9] on the ratio of base current increase to collector current decrease were extended to allow application to experimental data.

An empirical expression was developed for the space-charge volume damage introduction rate using data taken on specially fabricated devices. This expression gives reasonable predictions for fluences between 5×10^{14} and 10^{15} neutrons/cm^2 (E>10keV). Additionally, for matched devices the effect of the junction electric field strength is introduced through another experimentally derived expression which gives a reasonable fit for the same fluences and electric field strengths from 10^4 to 10^5 V/cm.

The agreement for all devices between Equation (23) and the experimental data from 5×10^{14} to 10^{15} neutrons/cm^2 indicates that the method presented for the separation of surface effects and neutron-induced bulk space-charge effects is valid.

The three matched devices showed an anomalous increase in collector current. This unexpected increase in collector current could have affected the electric field strength correlation but, since each of the three matched devices

showed the same behavior in their collector currents, their correlation is felt to be valid.

Injection annealing during irradiation was considered as a possible explanation for the junction electric field dependence seen in K_V, but it alone was unable to predict all of the observations (zero and reverse bias). This observation was sufficient to conclude that some other mechanism was responsible for the electric field dependence of the damage introduction rate. The exact nature of the electric field dependence (whether the defect cluster or its capture cross-section is modified by the junction electric field) could not be determined and further work in this area is needed (see Section VII).

An attempt was made to determine the processes involved by using other investigators' injection annealing studies[18] (see Appendix). These studies indicated reaction orders of five. The magnitude of the reaction order indicates that the processes are too complex to determine using the techniques presented.

VI. CONCLUSIONS

This work has shown that the space-charge damage introduction rate depends on the electric field strength present in the device junction during irradiation. In general, the rate of S-CRV damage introduction, K_V, is seen to be an increasing function of the average electric field strength present during irradiation and a decreasing function of the total neutron fluence.

The method presented for the separation of the neutron and gamma effects should be applicable to any type of device that shows a portion of its electrical characteristics which are dominated by either neutron or gamma effects. However, it requires the measurement of device parameters over a relatively wide range of fluences because it is a graphical technique.

The previous theoretical work[4,9] on the ratio of base current increase-to-collector current decrease was extended to allow application to experimental data and the results were applied to devices with the special device code.

An empirical relation for the space-charge volume damage introduction rate as a function of neutron fluence and junction electric field strength during irradiation was developed which gives reasonable predictions for fluences between 5×10^{14} and 10^{15} neutrons/cm^2 (E>10keV) and for junction electric field strengths 10^4 and 10^5 V/cm.

VII. SUGGESTIONS FOR ADDITIONAL WORK

While the anomalous behavior of neutron-induced defect clusters in the high field space-charge region during formation has been shown to be dependent on the electric field strength in the junction[1-6,10], the physical mechanism (e.g., modification of the defect cluster or its capture-cross-section) responsible for these effects has not been determined and should be investigated. The nature of the defect cluster in neutral bulk material has previously been studied and several models proposed[15,16]. A theoretical study of the effect of adding a high electric field to these models may lead to an understanding of the physical mechanisms involved.

Another possible investigation is the determination of the relative permittivity as a function of neutron fluence. Gossick has noted[17] that the permittivity would be modified by the inclusion of spherical voids in the material. Measurements of the dielectric constant of neutral bulk and space-charge samples, (if a method could be found) as a function of neutron fluence might yield information on the processes involved.

VIII. APPENDIX: INJECTION ANNEALING

A. Introduction

The effect of carrier injection on the transient neutron-induced damage in silicon planar-epitaxial transistors has been studied by others[18,19]. The general effect reported is an acceleration of annealing with both carrier density and temperature. Sander and Gregory[18] reported that an annealing stage is observed in their 213°K curves at times less than 5×10^{-2} seconds which is attributed to a second order reaction.

If a simple irreversible chemical-type reaction process is assumed for the reaction between injected carriers and neutron-induced defects, then the annealing process would be dependent upon the temperature, the relative concentration of reactants, and the order of the reaction with respect to each reactant[20]. Knowledge of these dependencies, if they exist, could confirm or deny the above assumption and could lead to a better understanding of the defect structure.

B. Determination of Reaction Order and Activation Energy

Reaction Order. If the reaction between carriers and defects is modeled by a simple irreversible chemical-type reaction between carriers, C, and defects, D, the general reaction rate equation can be written as[20],

$$\log(-dc_i/dt) = \log(k_r) + \alpha \cdot \log(c_C) + \beta \cdot \log(c_D) \qquad (27)$$

where

c_C = concentration of carriers,

c_D = concentration of defects,

c_i = concentration of reactant of observation (i = C or D depending on which concentration parameter is held constant),

k_r = reaction rate constant,

α = order of reaction with respect to carriers, and

β = order of reaction with respect to defects.

The general method for determining k_r, α, and β is to hold the concentration of one reactant constant, through a buffer or a high concentration, and to measure the reaction product concentration as a function of time. A plot of $\log_{10}(-dc_i/dt)$ versus $\log_{10}(c_i)$ will yield as the slope the value of the reaction order with respect to reactant i and as the intercept the value of k_r. Here i refers to that reactant which is not held constant.

Activation Energy. The relation between the rate constant, k_r, and temperature is given by,

$$k_r = k_{ro} \cdot \exp(-E_A/kT).$$

The constant, k_{ro}, is the frequency factor and E_A is the activation energy. Converting Equation (28) to logarithmic form, we have,

$$\log_{10}(k_r) = \log_{10}(k_{ro}) - E_A/2.3kT \qquad (29)$$

It is apparent that a plot of $\log_{10}(k_r)$ versus 1/T will yield $E_A/2.3k$ from the slope and $\log_{10}(k_{ro})$ from the intercept.

C. Results

Experimental Techniques. The reaction order with respect to defects was calculated using data presented in Reference 18. The annealing factor, AF(t), is defined[18] as the ratio of the radiation-induced defect density at time t to the density of defects that do not anneal, i.e.,

$$AF(t) = \frac{\text{Number of Defects at Time = t}}{\text{Number of Defects at Time = } \infty} \quad . \qquad (30)$$

The annealing factor is determined from the measurement of a device parameter (in the referenced work[18], the common emitter current gain) as a function of time following the neutron irradiation. Allowing for the possibility of different introduction rates and different electrical effects for "annealable" defects (i.e., excess defects that anneal rapidly at room temperature) and "stable" defects[18], (i.e., room temperature stable defects) Equation (30) can be rewritten as,

$$AF(t) = \frac{A \cdot \Phi + B \cdot \Phi \cdot f(t)}{A \cdot \Phi + B \cdot \Phi \cdot f(\infty)} = \frac{A + B \cdot f(t)}{A + B \cdot f(\infty)} \qquad (31)$$

where

Φ = neutron fluence (neutrons/cm^2)

A = the product of the introduction rate of "stable" defects and their electrical damage effectiveness ($(\Delta h_{FE}/\text{Defect}) \times (\text{Defects/neutron})$),

B = the product of the introduction rate of "annealable" defects and their electrical damage effectiveness ($(\Delta h_{FE}/\text{Defect}) \times (\text{Defects/neutron})$), and

f(t) = the fraction of "annealable" defects at time, t, following neutron irradiation.

The factors A and B are assumed independent of both time and the total neutron fluence. The latter assumption probably is invalid for fluences much higher then those used in the referenced work.

Since $f(\infty) = 0$, Equation (31) can be rearranged to,

$$AF(t) = 1 + \frac{B}{A} \cdot f(t), \qquad (32)$$

therefore $(AF(t) - 1)$ is seen to be proportional to the concentration of "annealable" defects.

The concentration of injected carriers will be directly proportional to the collector current, I_C, and will remain constant with time for constant injection level. If the quantity $\log(-d(AF - 1)/dt)$ is plotted versus $\log(AF - 1)$, Equation (27), at constant temperature and injection level, then the order of the reaction with respect to defects, β, can be obtained from the slope. It should be noted here that the value of k_r, in Equation (27), will not be obtainable since $(AF - 1)$ is only proportional to the concentra-

Time (s)	I_C=2 μA		I_C=20 μA		I_C=200 μA		I_C=1 mA	
	AF	AF - 1	AF	AF - 1	AF	AF - 1	AF	AF - 1
10^{-4}	4.50	3.50	3.12	2.12	2.62	1.62	2.29	1.29
10^{-3}	2.89	1.89	2.29	1.29	1.88	0.88	1.70	0.70
10^{-2}	2.15	1.15	1.81	0.81	1.54	0.54	1.44	0.44
10^{-1}	1.64	0.64	1.44	0.44	1.35	0.35	1.28	0.28
10^{0}	1.30	0.30	1.22	0.22	1.20	0.20	1.16	0.16
10^{1}	1.15	0.15	1.12	0.12	1.08	0.08	1.07	0.07
10^{2}	1.08	0.08	1.06	0.06	1.04	0.04	1.02	0.02
10^{3}	1.02	0.02	1.00	0.0	1.00	0.0	1.00	0.0

Table 8. Annealing factor as a function of time for several injection levels at 300°K[18].

tion of defects.

Data Presentation. The data presented in Table 8 was smoothed by least squares fitting of the data to a third degree polynomial, and dc/dt was calculated from the polynominal.

Figure 8 is a plot of log(-d(AF - 1)/dt) versus log(AF - 1) for each of the injection levels used. These curves show two regions. The first region, for times less then 10^{-1} seconds, is linear with an average slope of 5.0. The second region, for times greater then 10^{-1} seconds, is non-linear. A normal chemical reaction process generally has reaction orders of one, two, and very rarely, three.

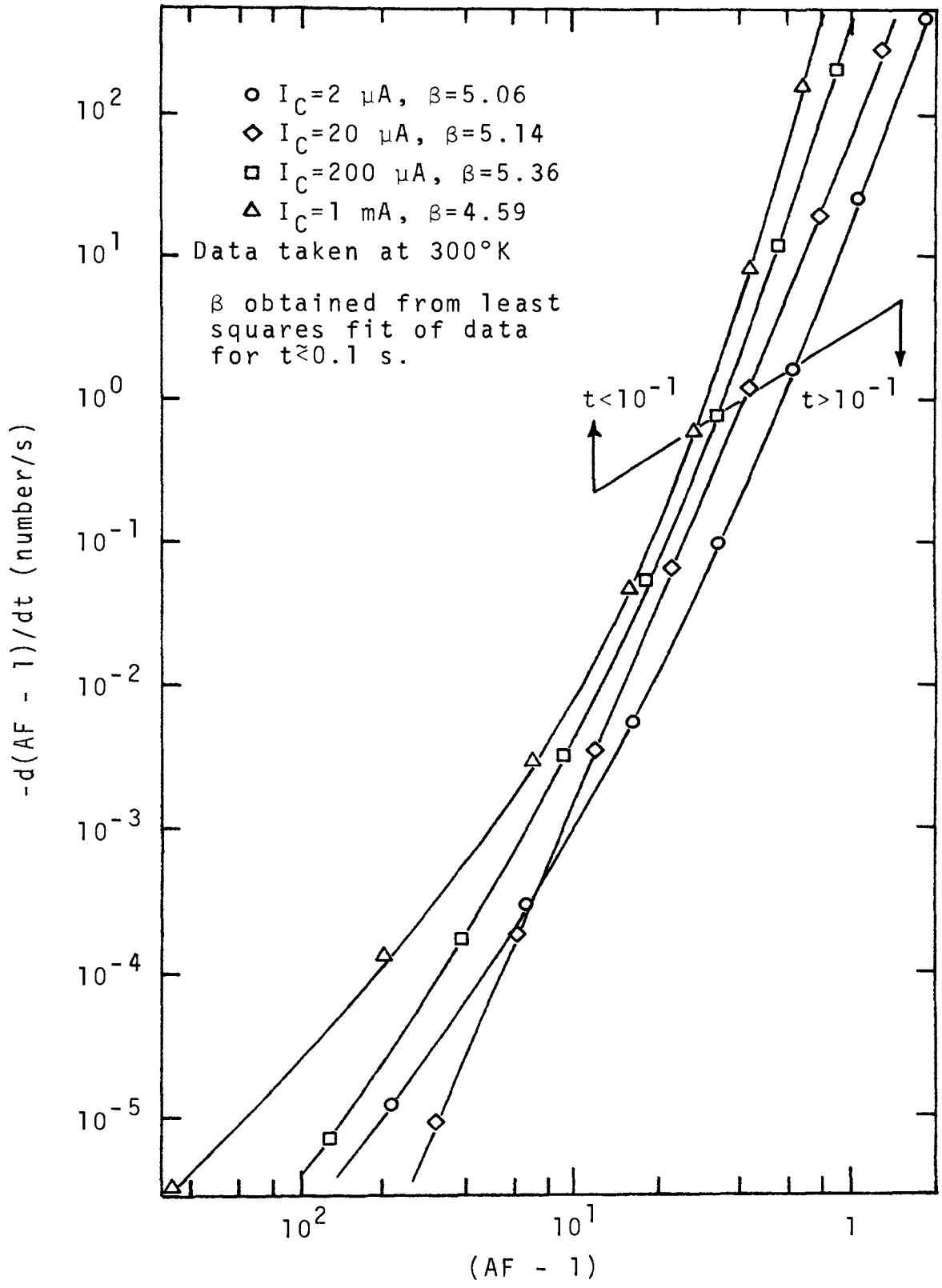

Figure 8. -d(AF - 1)/dt versus (AF - 1) for several collector currents with injection held constant.

D. Discussion

The resultant high value of the reaction order ($\beta = 5.0$) and the appearance of two different regions for each curve indicates that the reaction between carriers and defects is too complex to describe in terms of a simple irreversible chemical-type reaction. To obtain further results, the reaction processes involved would need to be determined, because the appropriate differential equation cannot be obtained without knowledge of these reaction processes.

REFERENCES

1. C. A. Goben and F. M. Smits, "Anomalous Base Current Component in Neutron Irradiated Transistors", IEEE Radiation Effects Conference, Seattle, Washington, 1964. Also: Sandia Laboratory (Albuquerque, New Mexico), (Publication) SCR-64-195, 1964.

2. C. A. Goben, "Neutron Bombardment Reduction of Transistor Current Gain", Ph.D. Dissertation, Iowa State University Library, Ames, Iowa, 1965. Also: Sandia Laboratory (Albuquerque, New Mexico), (Publication) SCR-64-1373, 1964.

3. C. A. Goben, "A Study of the Neutron-Induced Base Current Component in Silicon Transistors", IEEE Trans. on Nuclear Science, NS-12; 5, 134-146, 1965.

4. C. A. Goben, F. M. Smits and J. L. Wirth, "Neutron Radiation Damage in Silicon Transistors", IEEE Trans. on Nuclear Science, NS-15; 2, 14-29, 1968.

5. J. R. Chott and C. A. Goben, "Annealing Characteristics of Neutron Irradiated Silicon Transistors", IEEE Trans. on Nuclear Science, NS-14; 6, 134-146, 1967.

6. L. S. Su, G. E. Gassner and C. A. Goben, "Radiation and Annealing Characteristics of Neutron Bombarded Silicon Transistors", IEEE Trans. on Nuclear Science, NS-15; 6, 95-107, 1968.

7. B. L. Gregory and H. H. Sander, "Injection Dependence of Transient Annealing in Neutron-Irradiated Silicon Devices", IEEE Trans. on Nuclear Science, NS-14; 6, 116-126, 1967.

8. A. B. Phillips, Transistor Engineering, McGraw-Hill Book Company, Inc., New York, New York, 1962.

9. J. Bereisa, Jr. and C. A. Goben, "Neutron Dependence of Neutral Base Region Recombination", IEEE Trans. on Nuclear Science, NS-17; 6, 317-324, 1970.

10. C. A. Goben, C. H. Irani and P. E. Johnson, "Neutron Fluence and Electric Field Strength Dependencies of the Rate of Volume Damage Introduction in Silicon P-N Junctions", IEEE Trans. on Nuclear Science, NS-16; 6, 43-52, 1969.

11. T. A. Niemeier, "Inversion Layer Growth by Gamma Radiation", Unpublished Research, University of Missouri-Rolla, 1969.

12. M. C. Chow, "Recombination Statistics for the Neutron-Induced Base Current Component", Ph.D. Dissertation, University of Missouri-Rolla Library, Rolla, Missouri, 1968.

13. M. C. Chow, J. L. Azarewicz, and C. A. Goben, "Recombination Statistics for Neutron Bombarded Silicon Transistors", IEEE Trans. on Nuclear Science, NS-15; 6, 88-94, 1968.

14. C. A. Goben, Unpublished Research, University of Missouri-Rolla, 1971.

15. D. S. Billington and J. H. Crawford, Radiation Damage in Solids, Princeton University Press, Princeton, New Jersey, 1961.

16. J. H. Crawford, Jr., Interactions of Radiation with Solids, Plenum Press, New York, New York, 107-132, 1967.

17. B. R. Gossick, "Disordered Region in Semiconductors Bombarded by Fast Neutrons", Journal of Applied Physics, 30; 8, 1214-1218, 1959.

18. H. H. Sander and B. L. Gregory, "Transient Annealing in Semiconductors Devices Following Pulsed Neutron Irradiation", IEEE Trans. on Nuclear Science, NS-13; 6, 53-62, 1966.

19. M. Frank and F. Larin, "Effect of Operating Conditions and Transistor Parameters on Gain Degradation", IEEE Trans. on Nuclear Science, NS-12; 5, 126-133, 1965.

20. G. W. Costellan, Physical Chemistry, Addison-Wesley Publishing Company, Inc., Reading, Massachusetts, 1964.

ACKNOWLEDGEMENTS

The author wishes to express his appreciation to his advisor, Dr. Charles A. Goben, for his assistance in guiding this Master's thesis. Appreciation is also expressed to Dr. Albert E. Bolon and Dr. Fred C. Hardtke for their many useful suggestions and efforts in reading this thesis.

The author wishes to acknowledge the many useful and informative suggestions and discussions of his co-workers.

A special note of thanks goes to Mr. C. R. Jenkins for his valuable assistance.

The author expresses his appreciation to the United States Atomic Energy Commission and the Graduate Center for Materials Research of the University of Missouri-Rolla for their support of this research effort under contract AT(11-1)-1624. Texas Instruments fabricated the special devices used in these experiments.

To my wife, Sally, I owe the greatest measure of appreciation for the many hours spent in typing this thesis and for her patience and understanding.

VITA

Paul Edward Johnson was born on February 11, 1944 in St. Louis, Missouri and received his primary and secondary education in the Ritenour School District of Overland, Missouri. He received his Bachelor of Science in Metallurgical Engineering with Nuclear Option in January of 1967 at the University of Missouri-Rolla. He is a member of Scabbard and Blade.

The author worked for Alco Valve, St. Louis, Missouri during the summers of 1962-1966.

From July 1967 to the present, except for two years service in the United States Army (Europe), the author has been employed as a graduate research assistant working in the area of nuclear radiation effects on semiconductor devices at the Graduate Center for Materials Research of the Space Science Research Center, University of Missouri-Rolla.